JOURNAL OF VIROLOGY, May 1991, p. 2402–2407
0022-538X/91/052402-06$02.00/0

Vol. 65, No. 5

Delay Time for Influenza Virus Hemagglutinin-Induced Membrane Fusion Depends on Hemagglutinin Surface Density

MICHAEL J. CLAGUE,† CHRISTIAN SCHOCH,‡ AND ROBERT BLUMENTHAL*

Section of Membrane Structure and Function, National Cancer Institute, Building 10, Room 4B56, Bethesda, Maryland 20892

Received 22 October 1990/Accepted 6 February 1991

We have studied the kinetics of low-pH-induced fusion between erythrocyte membranes and membranes containing influenza virus hemagglutinin by using assays based on the fluorescence dequenching of the lipophilic dye octadecylrhodamine. Stopped-flow mixing and fast data acquisition have been used to monitor the early stages of influenza virus fusion. We have compared this with the kinetics observed for fusion of an NIH 3T3 cell line, transformed with bovine papillomavirus, which constitutively expresses influenza virus hemagglutinin (GP4f cells). Virus and GP4f cells both display a pH-dependent time lag before the onset of fluorescence dequenching, but of an order of magnitude difference, ca. 2 s versus ca. 20 s. We have adopted two strategies to investigate whether the difference in lag time reflects the surface density of acid-activated hemagglutinin, able to undergo productive conformational change. (i) Hemagglutinin expressed on the cell surface requires proteolytic cleavage with trypsin from an inactive HA0 form; we have limited the extent of proteolysis. (ii) We have used infection of CV-1 cells with a recombinant simian virus 40 bearing the influenza virus hemagglutinin gene. The surface expression of hemagglutinin is a function of time postinfection. For low-pH-induced fusion of both types of cell with erythrocytes, the lag time decreases with increasing hemagglutinin densities. Our results do not indicate a cooperative phenomenon at the level of the principal rate-determining step. We also show in the instance of virus fusion, that the magnitude of the delay time is a function of the target membrane transbilayer lipid distribution. We conclude that for a given amount of pH-activated hemagglutinin per unit area of membrane, the kinetics of fusion is determined by nonspecific physical properties of the membranes involved.

A key element of the infection pathway of many enveloped viruses is a low-pH-induced fusion of its membrane with that of a cell, somewhere along the endocytic pathway (17, 19). A considerable literature now exists documenting assays of fusion with more accessible membranes, in which the fusion event can be regulated by control of the buffer pH. For the well-studied case of influenza virus, the pH dependence of fusion has been shown to correlate with that of a conformational change of its spike glycoprotein, hemagglutinin (HA) (4, 15).

In this study, we use a fluorescence assay to monitor the time course of fusion, following reduction of the pH. The lipophilic dye octadecylrhodamine (R18) is initially incorporated into the viral membrane at self-quenching concentrations; fusion leads to dilution and hence an increase in fluorescence (10). The method was extended to monitor fusion of erythrocytes with a subclone of an NIH 3T3 cell line, transformed with bovine papillomavirus, which constitutively expresses HA (GP4f) (5). Kinetic studies of GP4f cell-erythrocyte fusion give evidence of a clear difference from influenza virus-virus-erythrocyte fusion, in that its onset is preceded by an easily measurable lag time of about 20 to 30 s at 37°C (13, 14). Using the R18 assay in conjunction with the stopped-flow technique, we have demonstrated (2, 3) a much shorter, pH-dependent lag for the fusion of vesicular stomatitis virus with erythrocyte ghosts. In this paper we demonstrate a similar phenomenon for influenza virus-erythrocyte ghost fusion which we compare with that seen for NIH 3T3 cells.

The HA expressed on the NIH 3T3 cell surface differs from that on virus in that it has not undergone proteolytic processing of its inactive HA0 form. However, HA0, which cannot undergo productive low-pH conformational change, can readily be converted to HA by treatment with trypsin. By varying this trypsin treatment, we have been able to vary the HA/HA0 ratio on the cell surface, while keeping the HA-plus-HA0 content constant. This has allowed an investigation of the time lag before onset of fusion as a function of HA surface concentration. As an alternative means of varying the cell surface density of HA, we have infected CV-1 cells with a recombinant simian virus 40 (SV40) virus bearing the HA gene (7). We then take advantage of the time-dependent expression of HA after infection, fully activating all HA at the surface by trypsin treatment. Both methods clearly show decreasing delays prior to fusion with increasing amounts of HA on the cell surface. Understanding the relationships between surface density of viral proteins and fusion is of major importance if we are to relate direct assays of viral fusion to the commonly used syncitium assays of cell fusion.

MATERIALS AND METHODS

Cell cultures. A subclone (GP4f) of a line of bovine papillomavirus-transformed NIH 3T3 cells that constitutively expresses HA from the influenza virus strain A/Japan/305/57 (H2N2) was grown as described previously (13). CV-1 (green monkey kidney) cells were obtained from the American Type Culture Collection and were cultured at 37°C in 5% CO_2 to 80% confluency in Dulbecco modified Eagle

* Corresponding author.
† Present address: European Molecular Biology Laboratory, D-6900 Heidelberg, Federal Republic of Germany.
‡ Present address: Institute of Medical Microbiology, CH-3010 Bern, Switzerland.

medium (DMEM) supplemented with 10% heat-inactivated calf serum (DMEM$^+$; GIBCO).

Infection of CV-1 cells with recombinant SV40-HA. Recombinant SV40-HA (SVEHA3) was kindly provided by M.-J. Gething and J. Sambrook, University of Texas, S.W. Medical Center. Passage 3 virus was used for all experiments. A 100-μl aliquot of virus stock suspension was used to infect a 75-cm^2 monolayer. The cells were washed once with DMEM, and the virus suspension was dropped onto the cells so that the whole surface was wetted. Subsequently, 3 to 4 ml of DMEM was added and the cells were incubated for 1 h at 37°C, with occasional rocking. Finally, 10 ml of prewarmed DMEM$^+$ was added. Approximately 80% of the cells were infected by this procedure, as judged by microscopic determination of erythrocyte binding 48 h postinfection. At different times postinfection, cell samples were prepared for the fusion assay in a similar manner to that for the GP4f cells with regard to neuraminidase treatment and erythrocyte binding. Activation and lifting were performed with 1 ml of trypsin-EDTA (0.5 mg of trypsin per ml, 0.2 mg of EDTA per ml) in Dulbecco phosphate-buffered saline (PBS; GIBCO) for 3 min at 37°C. This treatment ensured complete cleavage of surface HA0 as judged by Western immunoblotting. The reaction was stopped by addition of 1 ml of DMEM$^+$ followed by 12 ml of PBS. The cells were pelleted and washed in PBS.

Differential trypsin treatment of cells. A monolayer of cells grown in a 75-cm^2 flask was washed twice with DMEM and then incubated for 10 min at 37°C with 5 ml of DMEM containing 0.4 U of neuraminidase (type V from *Clostridium perfringens*; Sigma) per ml. It was then washed once with DMEM$^+$ and twice with DMEM. At this point, cells were incubated with 1 ml of DMEM containing 1 μg of *N*-tosyl-L-phenylalanine chloromethyl ketone (TPCK)-treated trypsin for various periods (90 to 720 s) at room temperature. Then 10 ml of DMEM$^+$ containing 0.6 mg of soybean trypsin inhibitor per ml was added. As a control, representing full trypsin cleavage, a monolayer was incubated for 10 min with 5 μg of trypsin at 37°C. Cells were washed twice with 10 ml of PBS. Then 5 ml of a suspension of erythrocytes in PBS (10^6/ml) was added and left for 3 min at room temperature, and then the mixture was washed twice with PBS. Under these conditions, most GP4f cells were left with one or two erythrocytes attached. Cells were then lifted by incubation for 10 min at 37°C with 1 ml of PBS containing 50 μg of *N*-tosyl-L-lysine chloromethyl ketone (TLCK)-treated chymotrypsin (which does not cleave HA0) per ml and 0.2% EDTA. These cells were washed once in PBS by centrifugation and subsequently kept at 4°C until a fusion assay was performed. The procedure for CV-1 cells differed slightly at the trypsin incubation step. Times and concentrations used are given in the relevant figures.

Estimation of degree of trypsinization of HA on GP4f cells and of its expression in CV-1 cells. Samples from cell fusion experiments were stored frozen at −70°C before characterization. Thawed samples were pelleted and then lysed in PBS containing 1% Triton X-100 at 4°C. After spinning at 10,000 × *g* for 10 min, the supernatant was collected and diluted 1:1 with 2× electrophoresis sample buffer consisting of 4% SDS, 50 mM Tris, 200 mM dithiothreitol, 40% glycerol, pH 6.8. Sodium dodecyl sulfate-polyacrylamide gel electrophoresis (SDS-PAGE) was performed by using a 12.5% Laemmli gel, after which proteins were transferred to nitrocellulose (pore size, 0.2 μm) by application of a potential of 40 V for 4 h. The nitrocellulose was "blocked" with 5% milk in PBS for 12 h at 4°C, after which 150 μl of rabbit serum containing anti-HA immunoglobulin G was added, diluted in 15 ml of the milk solution. After 2 h of gentle rocking at room temperature, the nitrocellulose was given four 15-min washes with fresh milk solution (25 ml). A milk solution containing iodinated protein A was then applied for 1 h at room temperature; this was followed by four more washes. Kodak X-Omat film at −70°C was then exposed to the nitrocellulose for various times. The degree of trypsin cleavage of HA0 on GP4f cells was estimated by comparing the ratio of the intensity of this band with that of HA1. Because the quantity of HA molecules per GP4f cell is known (6), a known quantity of these cells served as a reference for judging the expression of HA in CV-1 cells.

Preparation of erythrocyte ghosts. Resealed erythrocyte ghosts were produced by the procedure used by Clague et al. (2) based on that of Williamson et al. (18). The presence of Ca^{2+} in the lysis buffer destroys the asymmetric distribution of the erythrocyte membrane phospholipids (18).

Labeling of virus and binding to erythrocyte ghosts. Influenza virus, X31 strain, was produced in this laboratory by A. Puri. After collection from fertilized eggs, the virus was purified by centrifugation through a sucrose density gradient. The final concentration of virus was 1 mg of protein per ml. Three microliters of R18 solution (1 mg/ml) in ethanol was added to 1 ml of virus solution with rapid vortexing. After incubation for 10 min at room temperature, free R18 was removed by elution of the labeled influenza virus from a Sephadex G-25 PD10 column (Pharmacia, Piscataway, N.J.). The labeled virus was then incubated for 40 min at 4°C with 5 ml of ghost suspension, containing 3×10^9 ghosts as determined by a Coulter Multisizer. The suspension was then washed twice in PBS and stored as a resuspended pellet in 2 ml. Prior to the start of a series of stop-flow measurements, this solution was diluted about 40-fold in PBS.

Labeling of erythrocytes. A 30-μl aliquot of R18 solution (1 mg/ml) was added, with rapid vortexing, to 3 ml of suspension containing 10^9 washed erythrocytes in PBS. After 20 min at room temperature, 25 ml of DMEM$^+$ was added and left for an additional 20 min, and then the cells were spun down and washed five times with PBS.

Fluorescence monitoring of fusion kinetics. An SLM 8000 spectrofluorimeter (SLM Instruments Inc., Urbana, Ill.) was used for all experiments. Excitation and emission wavelengths were 560 and 590 nm, respectively. Cell-erythrocyte fusion assays were done in slow-kinetics mode, with untrypsinized cells complexed with erythrocytes as a control. Prewarmed cells were added to a thermostated cuvette containing PBS-citrate at the desired pH. Virus-erythrocyte fusion assays were either performed in fast-kinetics mode with an SFA-11 Rapid Kinetics Accessory (Hi-Tech Scientific Ltd., Salisbury, United Kingdom), or in slow-kinetics mode at reduced temperature (30°C). For rapid-kinetics measurements, the contents of two syringes were combined 1:1 to give the desired reaction mixture. One syringe contained R18 influenza virus-ghost suspension; the other held PBS plus sufficient citrate to produce the desired pH of the mixture. The observation cell was filled with freshly mixed thermostated suspension in about 50 ms, and the subsequent fluorescence intensity was monitored with 50-ms time resolution. Nine data sets were averaged for each fast-kinetics condition reported.

RESULTS

Figure 1A shows the early time course of R18 dequenching due to fusion of labeled influenza virus virions with erythro-

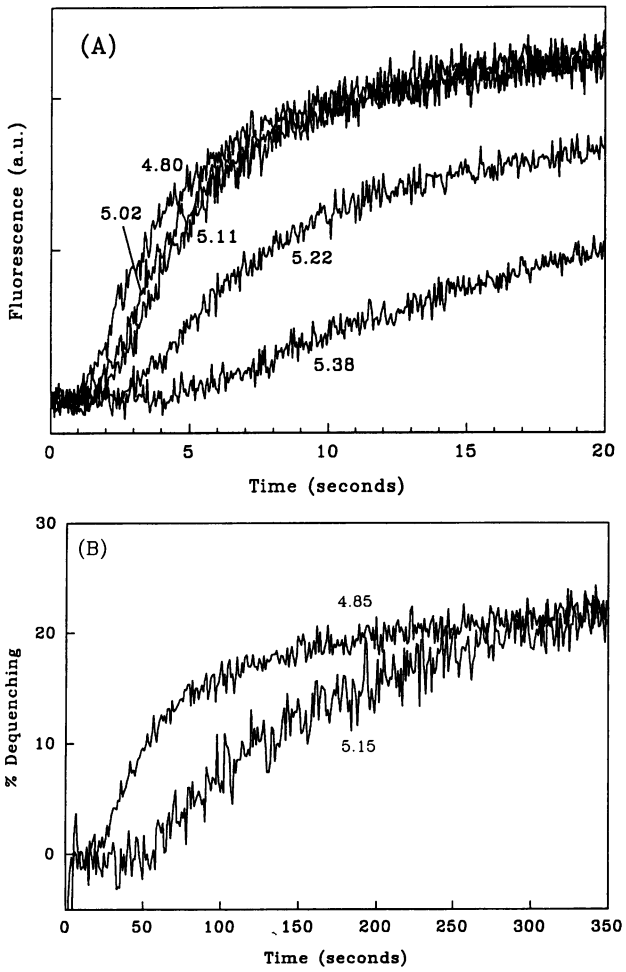

FIG. 1. (A) Rapid kinetics of fluorescence changes (in arbitrary units [a.u.]) upon fusion of R18-labeled influenza virus with erythrocyte ghosts. The reaction was triggered by rapid mixing of equal volumes of an R18-influenza virus-ghost suspension and a PBS-citrate solution as described in Materials and Methods. Nine data sets were averaged for each pH indicated in the figure. The temperature was 37°C. (B) Fluorescence dequenching kinetics of R18-labeled erythrocytes prebound to GP4f cells (fully trypsinized). Cells prewarmed at 37°C for 5 min were added at 0 s to PBS-citrate buffer at the pH indicated for each curve.

cyte cell ghosts. A familiar pH-dependent pattern of dequenching is obtained (16), but with the additional detail of a measurable pH-dependent lag time before it starts. This decreases with decreasing pH from about 4 s at pH 5.38 to a minimum of 1 s at pH 4.8. A considerably longer (>20-s) lag time is observed for fusion between GP4f and intact erythrocytes, as previously reported (13). Above pH 5.1 we observed a noticeable increase in this delay (Fig. 1B), reaching about 60 s at pH 5.15. An increase in delay correlates with a subsequently lower rate of R18 dequenching (2), and we are therefore just about at the limit of our resolution at this higher pH value because we require a fairly sharp discontinuity in the fluorescence signal with time to be able to estimate the delay with any precision (for these experiments we had lower extents of fusion than for the trypsin experiments shown in Fig. 3, with which we can resolve longer lag times).

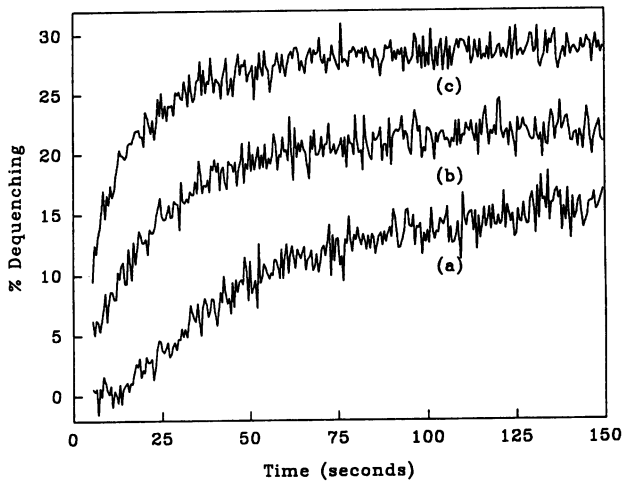

FIG. 2. Fluorescence-dequenching kinetics for R18-labeled X31 influenza virus prebound to intact erythrocytes (curve a) and resealed ghosts with asymmetric (curve b) and symmetric (curve c) phospholipid distributions. Prewarmed virus-cell complexes were injected into PBS-citrate (pH 4.9) at 30°C.

The stopped-flow viral fusion measurements used a ghost preparation having a symmetric phospholipid distribution as target membranes, whereas the GP4f cells were fused with intact erythrocytes. Figure 2 shows that for viral fusion at 30°C, the magnitude of the delay time is sensitive to the nature of the target membrane and thus the GP4f fusion delay times cannot be quantitatively compared with the stopped-flow derived values for virus fusion. At 30°C, fusion between virus and intact erythrocytes has a delay of about 12 s (Fig. 2), which decreases at 37°C to less than 4 s (data not shown), which is the earliest time point we record with stirrer mixing. Thus, the observed target membrane dependence does not account to any great extent for the large difference in delay times observed between virus and GP4f cell fusion at 37°C.

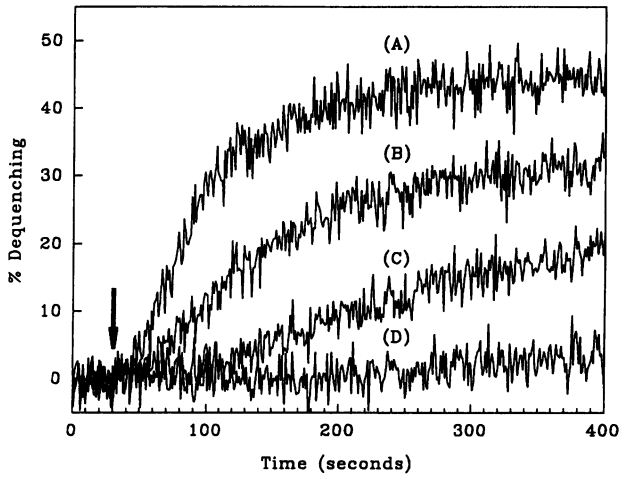

FIG. 3. Fluorescence dequenching kinetics of R18-labeled erythrocytes prebound to GP4f cells of different HA/HA0 surface ratios. At 30 s (arrow) the pH of the PBS (pH 7.4) buffer was reduced to 4.9 by injection of 0.3 M citrate. Curves A to D represent decreasing HA/HA0 ratios. The temperature was 37°C.

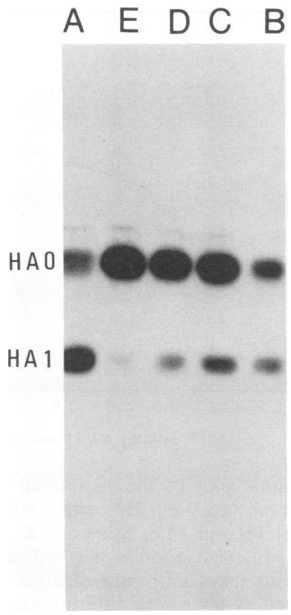

FIG. 4. Western blot of GP4f cells, for which corresponding fusion kinetics are shown in Fig. 3 (lanes A to D). Trypsinization conditions were 5 μg of trypsin per ml, 10 minutes at 37°C (A), 720 s (B), 360 s (C), 180 s (D), and 90 s (E). Lanes B to E were treated with 1 μg of trypsin per ml at room temperature. Lane B contains less material.

The kinetic consequences of limiting HA0 cleavage by trypsin for GP4f cell fusion at pH 4.9 are shown in Fig. 3. A typical Western blot used to estimate the degree of cleavage in this experiment is shown as Fig. 4. The antibody used is specific for the HA1 cleavage product, so we can therefore obtain our percentage cleavage by comparing the densities of the HA0 and HA1 bands in a given lane. The control (full trypsin treatment) indicates that 16% of total cellular HA (HA_{tot}) is not expressed at the cell surface, in good agreement with a study by Matlin and Simons (11). Total surface HA (HA_{surf}) thus equals HA_{tot} minus $0.16HA_{tot}$ and percentage cleavage of HA_{surf} equals ($HA1/HA_{surf}$) × 100.

Expression of HA on CV-1 cells increases with time post infection by the SV40 vector, maximal surface densities exceed that for GP4f cells. Our estimates of the time course and extent of HA expression obtained by Western blotting agree well with those obtained by Gething and Sambrook (8) using a radioimmunoassay. We obtained shorter delay times with increasing time postinfection between 20 and 48 h following full activation with trypsin. Differential trypsin treatment of CV-1 cells taken 24 h postinfection gave decreasing delay times with increased trypsin cleavage of HA0. Quantitation of the cell surface HA density dependence of the delay time is presented in Fig. 5, for all three means of variation used in our study (see Discussion).

DISCUSSION

In our assays we monitored the kinetics of fusion characteristic of a population of fusion events. This allowed us to rather easily determine the earliest point at which R18 dequenching can be recognized. This must correspond to the earliest point at which some degree of membrane continuity is established for a subpopulation of our fusing species. Curve-fitting or single-cell measurements would allow determinations of the distribution of delay times, but would suffer from difficulties in obtaining a unique solution to a correct multistate model and technical difficulties in acquiring sufficient data, respectively.

The kinetics of influenza virus-erythrocyte fusion have been previously studied by using the R18 assay (16). Lag times were not observed for virus prebound to ghost membranes at 37°C, because of the time resolution of both mixing and data acquisition. With decreasing pH, we obtained increasing initial rates of fusion to a maximal value (V_{max}) around pH 4.8. We have shown that a pH-dependent time lag precedes both influenza virus-erythrocyte ghost and GP4f/CV-1–erythrocyte fusion. The result for the virus is reminiscent of that previously reported for vesicular stomatitis virus fusion (2), whereas a pH dependence of the lag time for GP4f-red cell fusion contradicts results of previous work by Morris et al. (13). The reason for this disparity appears to be the mode of pH reduction. The procedure of Morris et al. (13) involves injection of a small volume of 0.3 M citric acid into a stirred cuvette containing the cells. Using their procedure, we also observed a pH-independent lag time (data not shown), which may be due to a population always experiencing a pH lower than the final pH during the mixing time (ca. 3 s) and thus proceeding at V_{max}. We should point out that we have used this mode of pH reduction in carrying out the experiments on GP4f fusion kinetics following limited HA0 cleavage (Fig. 3). We were able to do so because the comparison took place under identical acidification conditions and at a final pH value at which the minimum delay was obtained with the alternative method.

For reasons not yet understood, although the low-pH-induced conformation of HA is irreversible, the final amount of this form, as judged by proteinase K sensitivity and liposome binding, is pH dependent (4). As protonations of amino acid residues are rapidly reversible, we presume that there must be at least one competing pH-dependent pathway which precludes the conversion to the active form. We may therefore think of pH regulating the density of "fusion-active" HA on the membrane surface within a relevant time frame. Thus, it is attractive to ascribe both the difference between virus and GP4f/CV-1 lag times and their pH dependences to a function of the membrane surface density of HA (in fusion-competent conformation). This idea is borne out by the experiment in which the density of active HA on the GP4f surface is further varied by means of limited proteolytic cleavage, with longer lag times resulting from less cleavage. Further confirmation is given by the CV-1 experiments in which the delay becomes shorter as the number of HA trimers on the cell surface increases.

Figure 5 shows the collected data for the density dependence of the delay time at pH 4.9 for cell-erythrocyte fusion. It is unknown how many cleavages per trimer are required to render it fusion active; we therefore plot three limiting cases assuming a random trypsinization: (i) only fully cleaved trimers are fusion active (Fig. 5A); (ii) each HA0-to-HA cleavage contributes equally to the fusion process (Fig. 5B); and (iii) a single cleavage yields a fully active trimer (Fig. 5C). For the experiment in which density has been controlled by time postinfection, the results are unaffected by such considerations, as cleavage is maximal for each datum point. It is striking that Fig. 5A gives the most consistent set of slopes, as Boulay et al. (1) have shown that the HA conformational change is a cooperative phenomenon between trimer subunits. We have normalized each data set so that the fully cleaved sample (or the longest infected) is set to 100%. For GP4f cells, this has been estimated to correspond

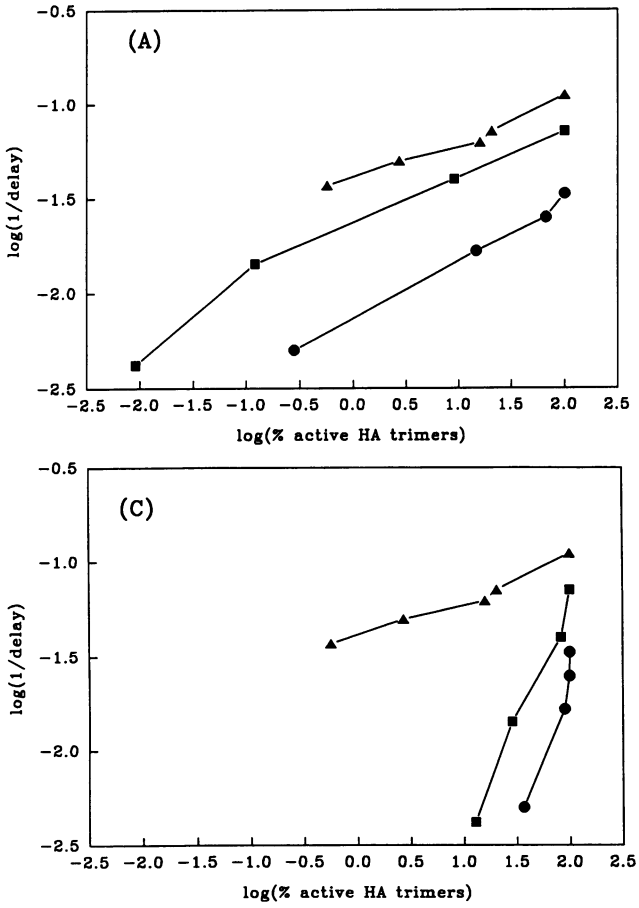

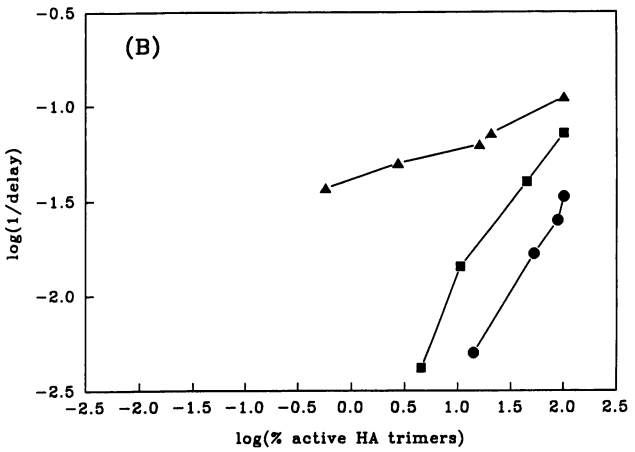

FIG. 5. Logarithmic plot of the reciprocal of estimated delay time versus the percent maximal HA active trimer expression (for each data set) at pH 4.9 and 37°C. Symbols: ▲, CV-1 cells infected with SV40-HA for different periods, all surface HA activated by trypsin; ●, CV-1 cells taken 24 h postinfection with SV40-HA and subsequently cleaved by trypsin to differing extents; ■, GP4f cells, surface HA cleaved to differing extents. Because the fusogenic capacity of a partially cleaved HA trimer is unknown, three cases are plotted assuming that our measured extent of cleavage represents a random process: only a fully cleaved trimer is active (A); each cleaved subunit independently makes one-third of the contribution of a fully cleaved trimer (B), and the cleavage of only one subunit fully activates a trimer (C).

to a trimer surface density of 1,600 μm^{-2} (6), but for CV-1 cells in suspension the membrane area is unknown. An estimate of the number of HA trimers expressed per CV-1 cell 48 h postinfection gave a number of 6.7×10^8, which presumably corresponds to a manyfold-higher HA density than that for GP4f (3.4×10^6 [6]). It is worth noting that although we have associated pH with changing active HA surface density, pH data cannot be directly used without knowledge of the number and pK_a of relevant protonatable groups; these values are currently unavailable.

Henis et al. (9) have shown that cell-cell fusion induced by Sendai virus envelope proteins is critically dependent on the surface concentration of laterally mobile viral protein. Moreover, Ellens et al. (6) have compared fusion efficiency, with liposomes bearing glycophorin, for two different cell lines, GP4f and HAb-2, of which HAb-2 expressed 1.9 times more HA but showed 4.4 times more fusion per bound liposome. From this, they concluded that more than one trimer is necessary for fusion, as previously suggested by a comparison between the pH profile for the extent of conformational change with that for the extent of cell-cell fusion (4). The comparatively shallow dependence of delay time on HA concentration (Fig. 5), irrespective of our assumptions of how many cleavages are required to activate a trimer, suggests that in these systems the establishment of membrane continuity is not rate limited by the formation of higher-order HA complexes. The results are consistent with the finding for GP4f cells that the extent of fusion at 37°C is determined within the first 10 s following pH reduction (13) during a pH-sensitive phase. This step, which constitutes one-third of the measured delay time, may contain the cooperative phenomenon evident from extent data such as that of Ellens et al. (6). Thus, our results do not exclude cooperativity between HA trimers in the fusion process; rather, they suggest that in the cell systems we have looked at, a cooperative process between HA trimers is not the major component of the delay. That the delay time for viral fusion is sensitive to manipulation of the lipid distribution in the erythrocyte membrane suggests a significant contribution by nonspecific factors. Hydrophobicity of both involved membranes may be important; phase-partitioning experiments have shown lipid-symmetric ghosts to be more hydrophobic than lipid-asymmetric ghosts (12), and also the hydrophobicity of the viral surface increases with density of fusion-active HA. Thus, we have shown that factors that increase the hydrophobicity of either membrane decrease the delay.

In summary, we have presented evidence that the actual surface density of active HA is a significant determinant of a time delay preceding acid-induced influenza virus HA-mediated membrane fusion. The pH dependence of the delay time can be attributed to this fact, as the extent of the requisite conformational change is itself pH dependent (4). Kinetic parameters probably do not offer the basis for determining the minimal number of HA trimers in fusion units, perhaps because they are recruited before rate-limiting steps.

ACKNOWLEDGMENTS

We thank Christina Cenciarelli for help with Western blotting, Ari Helenius for the gift of anti-HA, Judy White for GP4f cells, Mary-Jane Gething and Joe Sambrook for SV40 HA, and Robert Doms and Andreas Herrmann for helpful discussions.

REFERENCES

1. **Boulay, F., R. W. Doms, R. G. Webster, and A. Helenius.** 1988. Posttranslational oligomerisation and cooperative acid activation of mixed hemagglutinin trimers. J. Cell Biol. **106**:629–639.
2. **Clague, M. J., C. Schoch, L. Zech, and R. Blumenthal.** 1990. Gating kinetics of pH-activated membrane fusion of vesicular stomatitis virus with cells: stopped flow measurements by dequenching of octadecylrhodamine fluorescence. Biochemistry **29**:1303–1308.
3. **Clague, M. J., C. Schoch, L. Zech, and R. Blumenthal.** 1990. Stopped flow measurements of pH-activated membrane fusion of intact virus with cells. Biophys. J. **57**:494a.
4. **Doms, R. W., A. Helenius, and J. M. White.** 1985. Membrane fusion activity of the influenza virus haemagglutinin. J. Biol. Chem. **260**:2973–2981.
5. **Doxsey, S. J., J. Sambrook, A. Helenius, and J. M. White.** 1985. An efficient method for introducing macromolecules into living cells. J. Cell Biol. **101**:19–27.
6. **Ellens, H., J. Bentz, D. Mason, F. Zhang, and J. M. White.** 1990. Fusion of influenza hemagglutinin-expressing fibroblasts with glycophorin-bearing liposomes: role of hemagglutinin surface density. Biochemistry **29**:9697–9707.
7. **Gething, M.-J., R. W. Doms, D. York, and J. White.** 1986. Studies on the mechanism of membrane fusion: site specific mutagenesis of the hemagglutinin of influenza virus. J. Cell Biol. **102**:11–23.
8. **Gething, M.-J., and J. Sambrook.** 1981. Cell-surface expression of influenza hemagglutinin from a cloned DNA copy of the RNA gene. Nature (London) **293**:620–625.
9. **Henis, Y. I., Y. Herman-Barhom, B. Aroeti, and O. Gutman.** 1989. Lateral mobility of both envelope proteins (F and HN) of Sendai virus in the cell membrane is essential for cell-cell fusion. J. Biol. Chem. **264**:17119–17125.
10. **Hoekstra, D., T. de Boer, K. Klappe, and J. Wilschut.** 1984. Fluorescence method for measuring the kinetics of fusion between biological membranes. Biochemistry **23**:5675–5681.
11. **Matlin, K., and K. Simons.** 1983. Reduced temperature prevents transfer of a membrane glycoprotein to the cell surface but does not prevent terminal glycosylation. Cell **34**:233–243.
12. **McEvoy, L., P. Williamson, and R. A. Schlegel.** 1986. Membrane phospholipid asymmetry as a determinant of erythrocyte recognition by macrophages. Proc. Natl. Acad. Sci. USA **83**:3311–3315.
13. **Morris, S. J., D. P. Sarkar, J. M. White, and R. Blumenthal.** 1989. Kinetics of pH-dependent fusion between 3T3 fibroblasts expressing influenza hemagglutinin and red blood cells: measurement by dequenching of fluorescence. J. Biol. Chem. **264**:3972–3978.
14. **Sarkar, D. P., S. J. Morris, O. Eidelman, J. Zimmerberg, and R. Blumenthal.** 1989. Initial stages of influenza haemagglutinin induced cell fusion monitored simultaneously by two fluorescent events: cytoplasmic continuity and lipid mixing. J. Cell Biol. **109**:113–122.
15. **Skehel, J. J., P. M. Bayley, E. B. Brown, S. R. Martin, M. D. Waterfield, J. M. White, I. A. Wilson, and D. C. Wiley.** 1982. Changes in conformation of influenza virus hemagglutinin at the pH optimum of virus-mediated membrane fusion. Proc. Natl. Acad. Sci. USA **79**:968–972.
16. **Stegmann, T., D. Hoekstra, G. Scherpof, and J. Wilschut.** 1986. Fusion activity of influenza virus. A comparison between biological and artificial target membrane vesicles. J. Biol. Chem. **261**:10966–10969.
17. **White, J. M., M. Kielian, and A. Helenius.** 1983. Membrane fusion proteins of enveloped animal viruses. Q. Rev. Biophys. **16**:151–195.
18. **Williamson, P., L. Algarin, J. Bateman, H. R. Choe, and R. A. Schlegel.** 1985. Phospholipid asymmetry in human erythrocyte ghosts. J. Cell. Physiol. **123**:209–214.
19. **Yoshimura, A., K. Kuroda, K. Kawasaki, S. Yamashina, T. Maeda, and S. Ohnishi.** 1982. Infectious cell entry mechanism of influenza virus. J. Virol. **43**:284–293.